Online Assessment of Contact Erosion in High Voltage Gas Circuit Breakers based on different Physical Quantities

Milad Mohammadhosein, Kaveh Niayesh, *Senior Member, IEEE*, Amir Abbas Shayegani Akmal, and Hossein Mohseni

***Abstract*-- In this paper, an effort has been made to evaluate the online condition of arc contacts as a vital component of interruption chamber in high voltage puffer type SF_6 circuit breakers. The relationship between eroded mass caused by short-circuit current interruption and different thermal stress indices such as transferred electrical charge, current squared, and arc energy is investigated, by performing many experiments with different current amplitudes and arcing times. It is demonstrated that none of the known indices can solely determine mass erosion caused by the current interruption. Therefore, the equations including two of defined parameters are proposed to evaluate mass erosion. The method using arc energy and transferred electrical charge owns the highest accuracy in evaluating mass loss. However, considering the complexity of arc voltage measurements, a second method using current and arcing time can be also utilized. In addition, the development of erosion during the lifetime of arc contacts is studied. It is shown that arc roots tend to form on new uneroded areas of the contacts during current interruption, resulting in different erosion rates between the first few and subsequent interruptions due to change of morphology of the contacts after the first few switching operations.**

***Index Terms*-- online condition monitoring, arc contacts, contact erosion, thermal stress index, arc erosion development.**

I. Introduction

As power systems develop further, the demand for high-reliable circuit breakers with minimized operation and maintenance costs increases. This growing requirement is highly responsible for the shift from Time Based Maintenance (TBM) towards Condition Based Maintenance (CBM) and Reliability Centered Maintenance (RCM) [1]. In fact, utilities tend to do the costly maintenances, if necessary and only on those circuit breakers with the highest priority. In this approach, diagnostic techniques evaluating the condition of subcomponents play a significant role [2]. Among different methods of monitoring, online condition assessments took priority over all other methods owing to the fact that they are more compatible with growing presence of smart grids [3, 4].

Thanks to well-manufactured subcomponents of high voltage circuit breakers, the rate of major failures has decreased dramatically over the years. Three extensive surveys on high voltage equipment, including circuit breakers, carried out by CIGRE working groups during time periods of 1974-1977 [5], 1988-91 [6], and 2004-07 [7] indicate that the major failure frequency decreased from 1.6 failures per 100 circuit-breaker years in the first survey, to 0.7 in the second, and to 0.3 in the third [8]. On the other hand, from the standpoint of failure causes, 43 to 44% are attributed to mechanical system, 20 to 29% are concerned with auxiliary and control circuits, and 21 to 31% are related to high voltage component, where up to 14 percent of major faults are attributed to interruption chamber [9].

The dissipated energy in interruption chamber of gas circuit breakers during current interruption process is absorbed by contacts, nozzle and SF_6 as the arc quenching gas. The absorbed energy causes contacts and nozzle to heat, melt and finally vaporize, which is typically referred to as contact erosion and nozzle ablation. Contact erosion gradually decreases the length of the arcing contacts resulting in degradation of current interruption capability. In a severe case, it causes current not to commutate from main contacts to arcing contacts properly leading to a failed current interruption.

As a malfunction of the interruption chamber causes the circuit breaker not to manage to break short-circuit currents, condition monitoring of components of interruption chambers is considered as the highest priority [9].

Investigation on the number of successful interruption of short circuit currents, as electrical endurance, has been under consideration in the existing literature. The methods to evaluate the contact erosion and nozzle ablation can be divided into two major categories. In the first category, the methods are based on measuring some parameters to recognize the present state and the degree of contacts degradation. Vibration analysis based on measuring the acoustic emission [10, 11], and measuring the static and dynamic contact resistance [12-15] are considered in the first category. In the second category, the remaining lifetime is determined by considering the accumulated stress imposed to the interruption chamber components. In this context, an ongoing attempt has been made to define certain criteria indicating the mass loss of contacts during every interruption. Based on the available measured data, different methods have been proposed. In the simplest approach, solely the number of faults is counted. It is, however, not precise enough because

M. Mohammadhosein, A. A. Shayegani Akmal and H. Mohseni are with the School of Electrical and Computer Engineering, College of Engineering, University of Tehran, Iran. (e-mail: Mohammadhosein@ut.ac.ir)

K. Niayesh is with the Department of Electric Power Engineering, Norwegian University of Science and Technology, 7491 Trondheim, Norway.

different short circuit faults with various current amplitudes and arcing times, have a considerably different impact on interruption chamber components. In more accurate approaches, based on the availability of peak current amplitude, as in (1) [16]; based on the availability of instantaneous current during arcing time (transferred electric charge) in (2) [17]; and based on availability of arc voltage along with current waveform (arc energy) in (3) [18]; the remaining useful lifetime of interruption chamber is assessed.

$$N = \begin{cases} 1.83 \times \left(0.35 \times \frac{I_{scN}}{I_{sc}}\right)^3 & for\ I_{sc} < 0.35 I_{scN} \\ \left(0.5 \times \frac{I_{scN}}{I_{sc}}\right)^{1.7} & for\ I_{sc} \geq 0.35 I_{scN} \end{cases} \quad (1)$$

$$\Delta m_c = C(I_{rms}, \tau_{arc}) \times \int_{\tau_{arc}} |i(t)|\, dt \quad (2)$$

$$\Delta m_E = E \int_{\tau_{arc}} u(t).\, i(t)\, dt \quad (3)$$

Where N indicates the number of interruptions being supposed to have a similar contact erosion caused by one interruption at 50% of rated short circuit current (I_{scN}) for an SF_6 puffer type circuit breaker, I_{sc} is short circuit current, Δm_c is the mass loss calculated based on transferred electrical charge, $C(I_{rms}, \tau_{arc})$ is specific erosion depending on I_{rms}, the root mean squared value of the current, and the arcing time τ_{arc}. Δm_E is the mass loss calculated based on the arc energy, *E*, *u(t)*, and *i(t)* are a constant coefficient, the arc voltage and the arc current, respectively.

In equation (2), the ratio of mass loss to transferred electric charge is dependent on current amplitude, arcing time, contact geometry, and contact polarity [17]. In equation (3), It is assumed that there is a linear relationship between contact erosion and the arc energy [18].

This paper aims to present an experimental investigation on contact erosion of an SF_6 puffer type circuit breaker. For this purpose, many experiments with different arcing times and arc current amplitudes have been conducted to study the contact erosion development. It is demonstrated that the relationship between contact erosion and transferred electrical charge or arc energy cannot be considered as linear. To improve the accuracy of mass loss prediction, thermal stress indices with two known parameters are proposed. The proposed method can be assumed as a non-invasive online technique to estimate the interruption chamber remaining lifetime.

II. Experimental setup

Fig. 1, shows schematically the test circuit producing high current, which is commonly used for testing of high voltage circuit breakers in a current injection type synthetic test circuit.

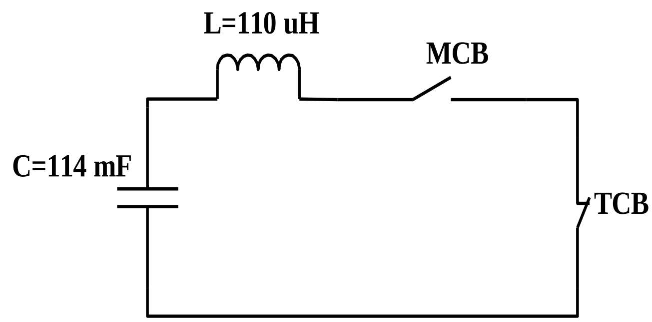

Fig. 1. The Schematic of the Test Circuit

In order to obtain various arcing times, it is required to know the operation times of the circuit breakers. The results of 15 no-load switching operations show that the average closing time of the making circuit breaker (MCB) is 56 ms, with a jitter smaller than 1 ms, and the average opening time of the test circuit breaker (TCB) is 42 ms with a jitter less than 2 ms.

The test starts by closing the MCB, which initiates the flow of the current. Based on the time difference between closing of MCB and opening of TCB, the test circuit breaker contacts are separated at a specific instant of the current and an arc is initiated. In fact, jitter indicates that the time delay between sending the close/open command to the circuit breakers and contact opening/closing does not remain a constant value, therefore this characteristic makes it difficult to conduct the experiments owning the same arcing time. The only way to achieve the same arcing time is to suppose the longest and the shortest probable delay of TCB and MCB, respectively. Based on this assumption, any difference in operation delay of circuit breakers causes the current not to flow through the circuit because the opening operation of the TCB precedes the closing operation of the MCB. In this method, the current flows if the opening and closing operations occur simultaneously, therefore the longest arcing time results.

Regarding low-amplitude resistance of the circuit and rated voltage of the capacitor bank, 2.6kV, the maximum current peak and frequency are 84 kA and 45 Hz, respectively.

Short-circuit currents have been applied on a 24 kV puffer type circuit breaker with short-circuit current rating of 25 kA. In order to measure the arc voltage and current, a capacitor divider having a ratio of 1000:1 and a 10 $\mu\Omega$-shunt resistor are used. In order to suppress the electromagnetic noise, the measured data are transmitted by a fiber optic link and stored in an oscilloscope with a sampling frequency of 500 kHz.

Regarding the well-known impact of contact shapes and dimensions on the erosion rates [19-21], every short circuit stress has been conducted on the same contact sets built with acceptable tolerance. In order to obtain acceptable accuracy in weight measurements, contacts were cleaned after each short-circuit interruption. Following each operation, the mass loss of contact sets was measured with a reasonable degree of accuracy. Figs. 2 and 3 show the experimental setup.

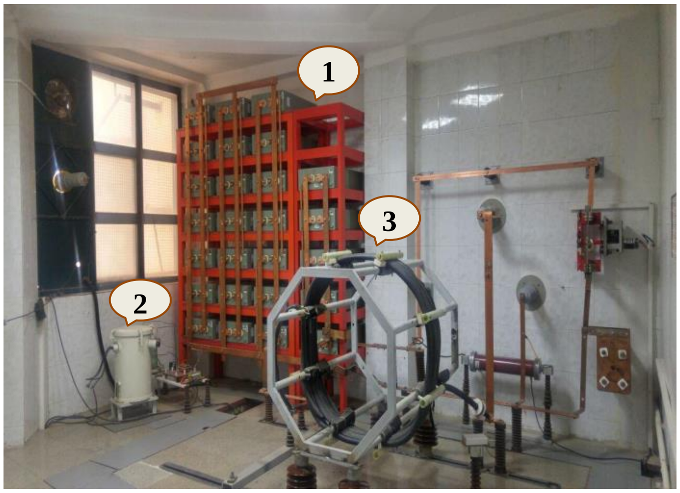

Fig. 2. Experimental Setup including: (1) Capacitor Bank, (2) Charging Circuit, (3) Reactor

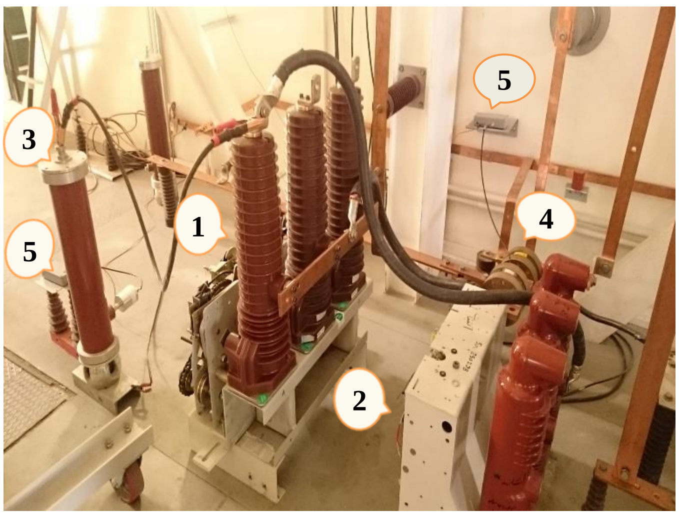

Fig. 3. Experimental Setup including: (1) TCB, (2) MCB, (3) Capacitor Divider, (4) Shunt Resistor, and (5) Optic Transmitter.

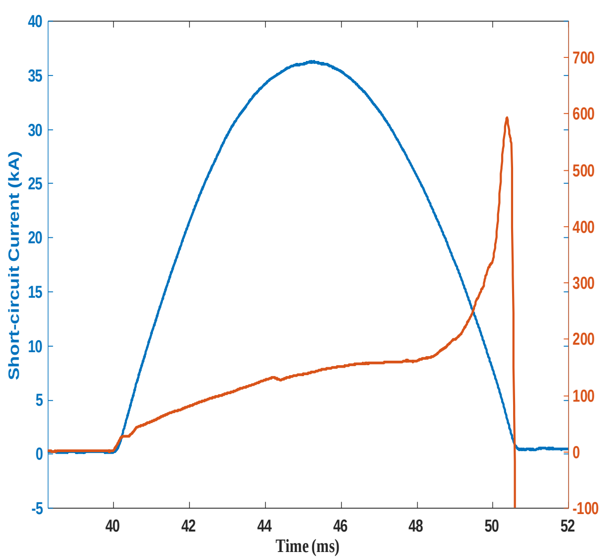

Fig. 4. The recorded short-circuit current and arc voltage waveforms

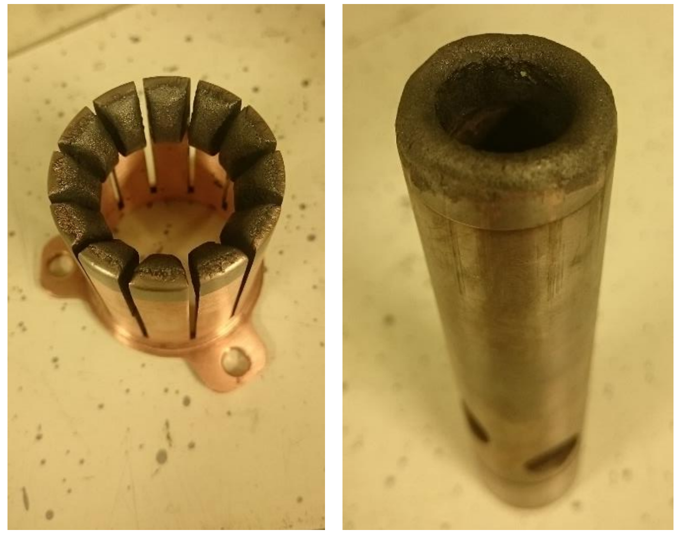

(a) (b)

Fig. 5. Eroded contact surfaces after interruption of a short circuit current of 37.5 kA (a) Moving Contact and (b) Fixed Contact

III. Measurement Results

Figure 4 shows the recorded arc voltage and arc current during the interruption of the rated short circuit current, 25 kA (RMS), with half-cycle arcing time. Figure 5 shows the moving and fixed contacts having been tested by a current of 1.5 times the rated short-circuit current and an arcing time of 22ms, whereas the current has been interrupted at the second zero-crossing point of the test current.

The experiments are divided into two main categories: varying the amplitude of current keeping the arcing time constant, and varying the arcing time when the current amplitude remains constant. Considering the dependency of contact erosion upon the shape and processing of the contacts, experiments have been carried out on the same contacts. According to the fixed common parameter, the experimental results are categorized into four distinct groups: experiments with common current amplitude, common arcing time, and approximately close values of transferred electrical charge and arc energy. The target has been to find out the relationship between the amount of material removed by arc erosion and measured variables; for instance, transferred electrical charge, integral of current squared during arcing time, and arc energy. In this study, the amount of mass loss as a function of mentioned variables is evaluated and it is shown that none of these variables can solely determine the contact mass loss.

A. Contact Mass Loss vs. Arcing Time

In order to investigate the impact of arcing time on the contact mass loss under short circuit current interruption, experiments with the same current amplitude (rated short-circuit current) have been carried out. Figure 6 demonstrates the measured mass loss variation after applying the current with specific arcing times of 5.64 ms, 7.94 ms, 8.77 ms, and 10.29 ms.

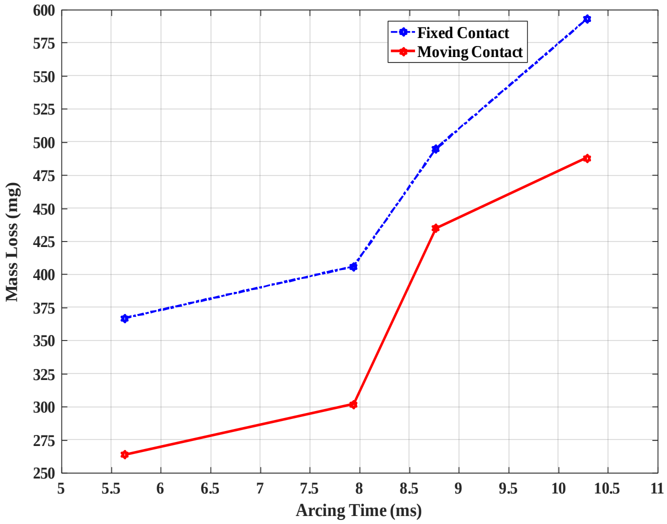

Fig. 6. Mass loss of fixed (anode) and moving (cathode) contacts as a function of arcing time at rated short-circuit current

In an approach, in order to evaluate the electrical endurance of a circuit breaker, the electrical arcing stress experienced by interruption chamber during short-circuit current interruption is assessed solely by known current amplitude. However, the results shown in Fig. 6 indicate that the contact erosion is highly dependent upon the contact polarity, contact geometry, and the arcing time. So that an increase in arcing time from 5.64 ms to 10.29 ms at specific current amplitude approximately doubles the amount of mass loss caused by the rated-short-circuit current interruption. On the other hand, the contact separation is likely to occur at any instant of the current waveform, so the presumption of constant arcing time for every short-circuit current appears unreasonable.

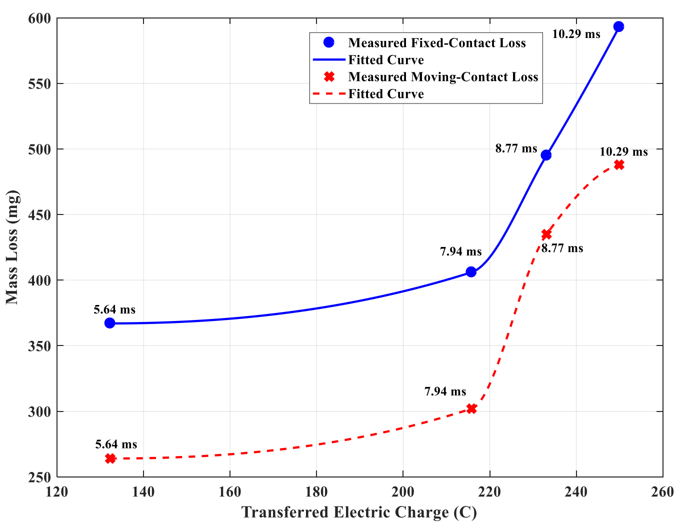

Fig. 7. Mass loss of fixed and moving contacts as a function of transferred electric charge at rated short-circuit current

In Fig. 7, Fig. 8, and Fig. 9, the amount of contact mass eroded by short-circuit current interruption is plotted as a function of transferred electrical charge, arc energy, and integral of current squared during arcing time, respectively.

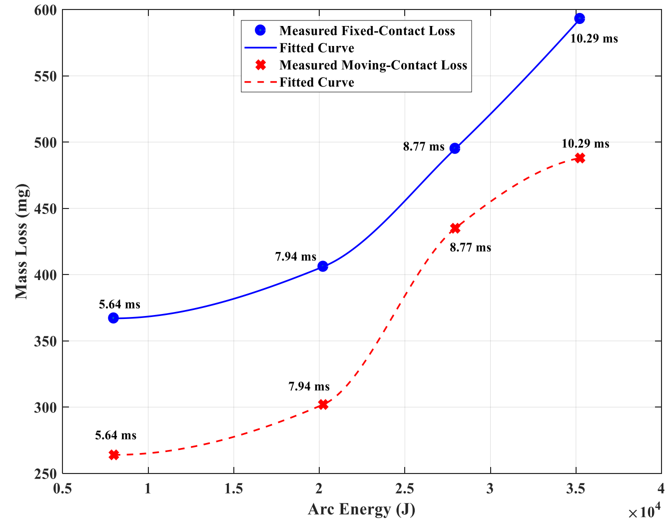

Fig. 8. Mass loss of fixed and moving contacts as a function of arc energy in rated short-circuit current

The plots show a steep increase in mass loss as a function of transferred electrical charge and squared current over high values of arcing time. For the case of fixed current amplitude and varied arcing time, results show that mass loss as a function of arc energy is more linear than other two defined quantities.

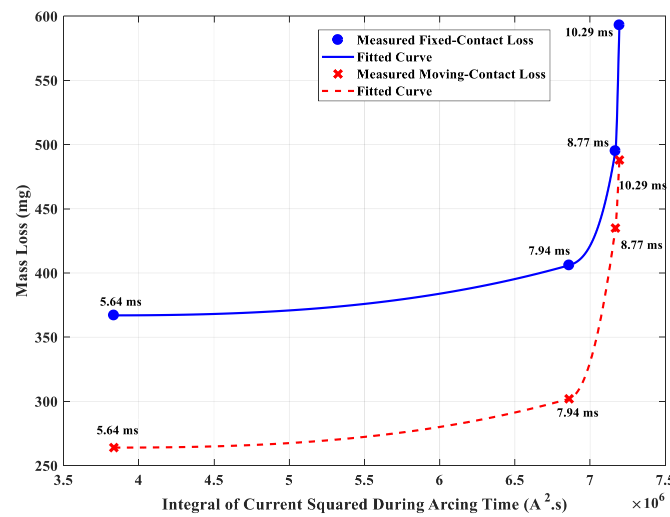

Fig. 9. Mass loss of fixed and moving contacts as a function of integral of current squared during arcing time at rated short-circuit current

B. Contact Mass Loss vs. Electrical Current

To study the behavior of mass loss erosion, the experiments have been done with current peak values of 13 kA, 20.9 kA, 28.6 kA, 33.4 kA, and 36.2 kA, and the arcing time keeping constant at half-cycle. Fig. 10, Fig. 11, and Fig. 12 demonstrate the mass erosion of electrodes during short-circuit current interruption as a function of transferred electrical charge, integral of current squared during arcing time, and arc energy, respectively. The plots show that in case of varying current amplitude at the fixed arcing time, electrical arc and integral of current squared have more linearly relationship than arc energy with mass loss.

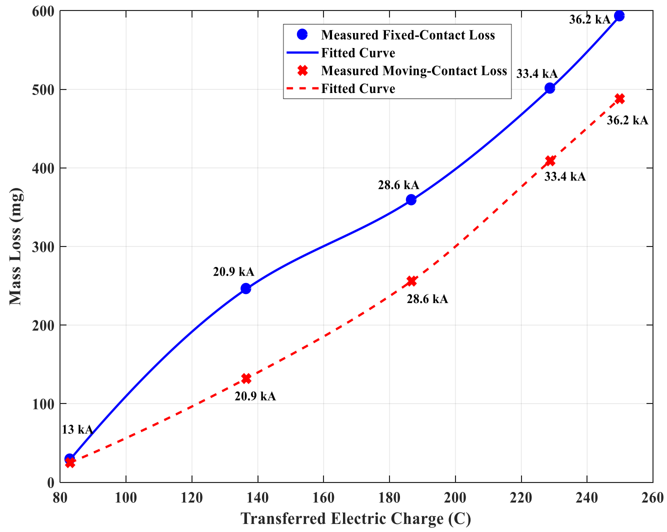

Fig. 10. Mass loss of fixed and moving contacts as a function of transferred electric charge at half-cycle arcing time

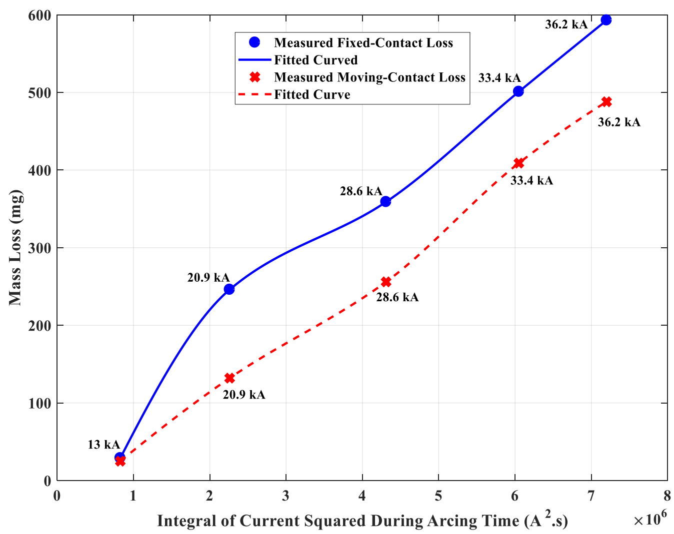

Fig. 11. Mass loss of fixed and moving contacts as a function of integral of current squared at half-cycle arcing time

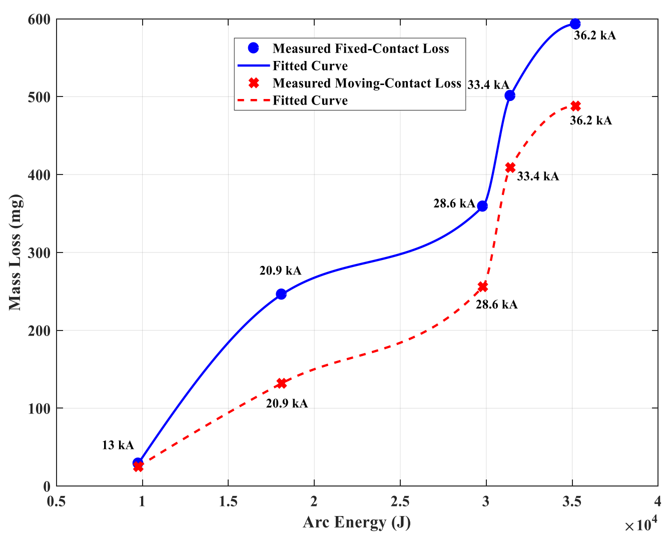

Fig. 12. Mass loss of fixed and moving contacts as a function of arc energy at half-cycle arcing time

There are three sets of data with approximately similar electrical quantities but considerably different contact erosions. Table I shows two experiments with approximately close transferred electrical charge; 132.3 C, and 136.5 C; but a considerable difference of contact erosion. The second data set represents an experiment with a greater amount of arc energy compared to another one; 29.8 kJ against 27.9 kJ; but notably less contact erosion. The third data set describes an experiment owning higher current squared measurement in comparison with another one, but a remarkable lower mass loss. The results confirm that none of the electrical quantities can solely be used to assess the amount of mass loss caused by the current interruption.

TABLE I
The Experimental Results Owning Approximately Close Thermal Stress Value but Considerably Different Mass Loss

Peak Current (kA)		Peak Current (kA)		Peak Current (kA)	
36.7	20.9	36.9	28.6	33.4	37.9
Arcing Time (ms)		Arcing Time (ms)		Arcing Time (ms)	
5.64	10.2	8.8	10.2	10.2	7.9
Transferred Electrical Charge (C)		Arc Energy (kJ)		Current Squared $((kA)^2.s)$	
132.3	136.5	27.9	29.8	6.05	6.86
Moving Mass Loss (mg)		Moving Mass Loss (mg)		Moving Mass Loss (mg)	
264	132	435	256	409	302
Fixed Mass Loss (mg)		Fixed Mass Loss (mg)		Fixed Mass Loss (mg)	
367	246	495	359	501	406

C. *Proposed Electrical index to Assess Mass Loss*

In order to gain a more accurate assessment of the eroded mass, the material loss can be defined as a function of two of the four well-known quantities, i.e., electrical current, arcing time, transferred electrical charge, and arc energy. Table II demonstrates the equations derived by considering all measured data including the experiments with varying current amplitude and constant arcing time, and vice versa. To specify how good the derived equations fit the measured data, the r-squared index was calculated. The closer the index is to one, the better is the model.

TABLE II
Proposed Equations Using Two Measured Electrical Parameters

Mass Loss / **Quantities**	**Moving Contact (mg)**	**Fixed Contact (mg)**
I_P(kA), T_a(ms)	$0.0047\ I_p^{2.354} T_a^{1.319}$	$0.0879\ I_p^{1.8} T_a^{0.992}$
R-squared	0.946	0.939
I_P(kA), Q_a(C)	$0.03\ I_p^{0.839} Q_a^{1.197}$	$0.347\ I_p^{0.755} Q_a^{0.841}$
R-squared	0.918	0.907
I_P(kA), E_a(kJ)	$0.1363\ I_p^{1.744} E_a^{0.527}$	$1.22\ I_p^{1.328} E_a^{0.379}$
R-squared	0.942	0.929
E_a(kJ), Q_a(C)	$0.014\ Qa^{2.041} E_a^{-0.241}$	$0.132\ Qa^{1.675} E_a^{-0.259}$
R-squared	0.893	0.874

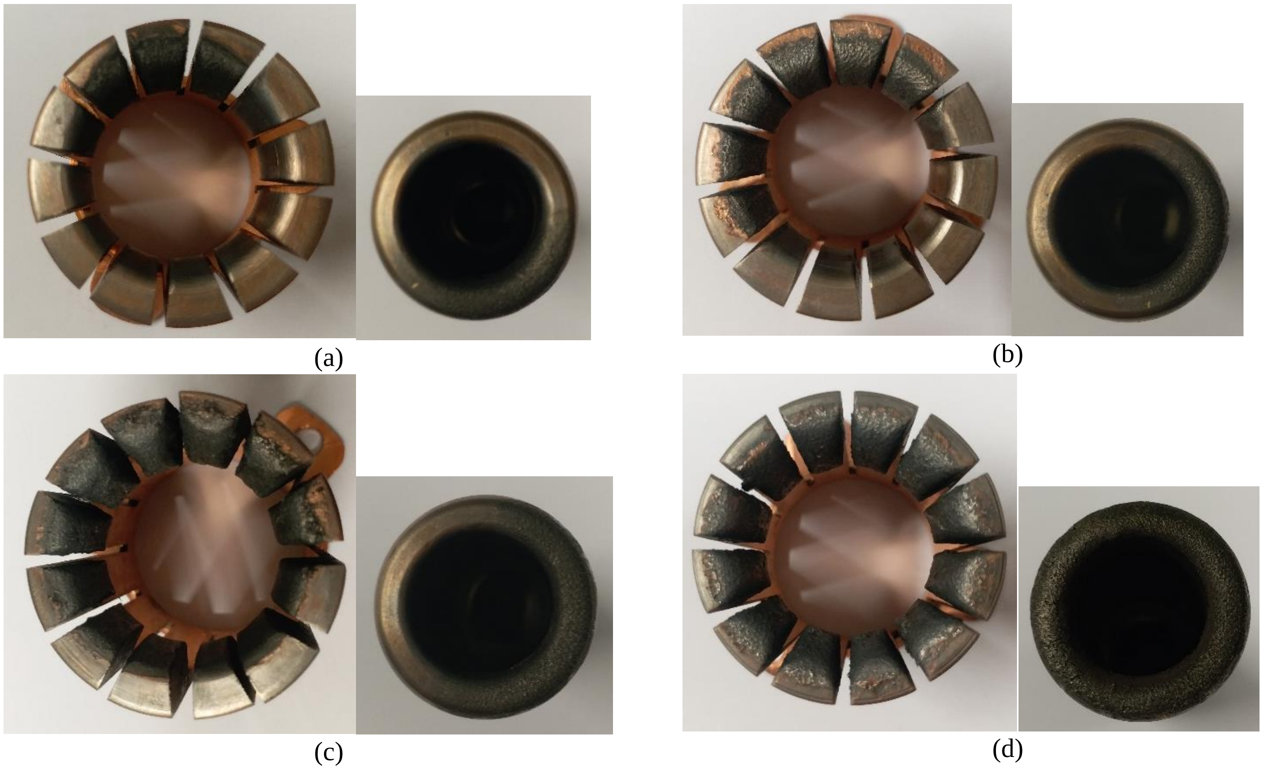

Fig. 13. Development of contact erosion during interruption of short-circuit currents after (a) one; (b) four; (c) eight; (d) 12 experiments with characteristics mentioned in table III.

D. Contact Mass Loss vs. Number of Operations

In order to have the same initial condition of contacts in each experiment, every short circuit current has been carried out on new replaced sets of contacts. Therefore, the validity of deduced equations between mass loss and electrical parameters during the lifetime of the circuit breaker is under question. In order to examine the mass loss versus the number of current interruptions, four series of tests including one experiment, four experiments, eight experiments, and twelve experiments have been carried out on the similar sets of contacts. The measured electrical parameters of the experiments given in Table III show that the thermal stress exerted on the interruption chamber is approximately similar during the experiments.

TABLE III

The electrical parameters of different series of experiments

	Arcing Time (ms)	$\int i\,dt$ (C)	$\int i^2 dt$ $((kA)^2.s)$	$\int i.v\,dt$ (kJ)
1	10.11	191.8	4.34	26.33
4	10.09, 10.16, 10.21, 10.16	196.5, 191.9, 195.4, 199.7	4.56, 4.37, 4.50, 4.67	25.73, 28.53, 26.42, 22.57
8	10.05, 10.20, 10.01, 10.22, 10.18, 10.25, 9.73, 10.01	191.6, 192.9 191.6, 195.1, 194.2, 194.1, 193.5, 194.6,	4.33, 4.33, 4.51, 4.45, 4.43, 4.39, 4.54, 4.40	29.68, 29.90, 25.74, 27.50, 28.06, 27.87, 25.21, 27.06
12	10.10, 10.16, 10.09, 9.83, 10.09, 10.02, 10.14, 10.15, 10.08, 10.22, 10.15, 10.21	188.8, 197.1 183.6, 190.2, 188.3, 190.1, 187.7, 185.1, 186.5, 188.1, 184.5, 195.5,	4.20, 3.98, 4.31, 4.22, 4.24, 4.14, 4.05, 4.09, 4.16, 4.01, 4.49, 4.55	25.57, 28.96, 23.28, 24.74, 25.38, 25.22, 26.62, 24.53, 22.97, 25.46, 27.52, 26.56

Fig. 13 showing the development of eroded areas of contacts during interruption of short-circuit currents. It provides a satisfactory explanation for the linear increase of contact erosion with the number of interruptions as shown in Fig. 14. In fact, arc roots tend to form on new uneroded remaining areas of the contact surface. Therefore, no matter how many current interruptions have been performed before, the erosion rate remains constant until the whole surface of contacts has been eroded. Afterward, the erosion rate decreases because during the previous interruptions the copper has become evaporated resulting in areas with more content of tungsten left on the surface of the contact. The higher thermal stability of tungsten in comparison with copper causes less amount of contact material to be eroded during consecutive short-circuit current interruptions.

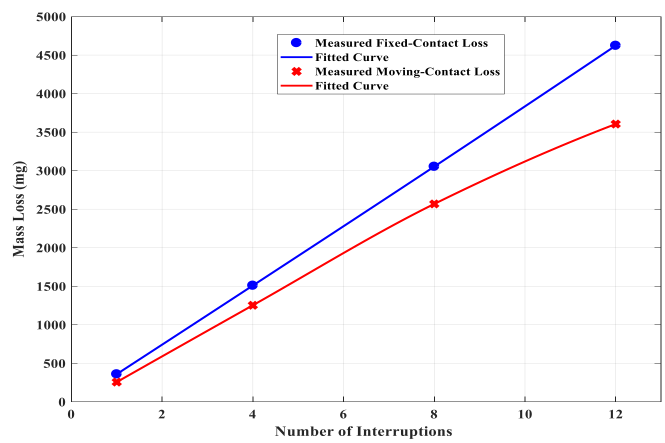

Fig. 14. Mass loss of fixed and moving contacts as a function of number of interruptions

TABLE IV
The electrical parameters of different series of experiments

Calculated Mass (mg) / Measured Mass (mg)		$M(I_p, T_a)$	$F(I_p, T_a)$	$M(I_p, Q_a)$	$F(I_p, Q_a)$	$M(I_p, E_a)$	$F(I_p, E_a)$	$M(E_a, Q_a)$	$F(E_a, Q_a)$
A_{Moving} 513	**A_{Fixed} 626**	451	708	515	768	532	804	540	772
B_{Moving} 790	**B_{Fixed} 1163**	707	995	722	1001	705	995	761	1023
R-squared		0.719	0.759	0.878	0.679	0.804	0.588	0.959	0.719

the copper has become evaporated resulting in areas with more content of tungsten left on the surface of the contact. The higher thermal stability of tungsten in comparison with copper causes less amount of contact material to be eroded during consecutive short-circuit current interruptions.

IV. Discussion

In order to assess the accuracy of the proposed equations in Table II, six experiments with data given in Table V have been carried out on two poles of the circuit breaker with new sets of contacts. As long as the whole surface of contacts after current interruptions is not eroded, based on the results shown in Fig. 14, the amount of mass loss for each contact set is supposed to be the sum of eroded masses during each of three short-circuit currents.

TABLE V
The electrical parameters of experiments carried out on phase A and phase B

Quantity / *Phase-Test NO.*	*I_P(kA)*	*T_a(ms)*	*Q_a(C)*	*E_a(kJ)*
A_1	24.8	8.01	145.98	19.04
A_2	23.2	9.00	149.83	26.77
A_3	23.8	9.20	150.44	21.59
B_1	29	7.61	155.52	14.04
B_2	28.1	10.37	187.98	27.83
B_3	27.8	10.24	182.89	25.36

According to the results presented in Table IV, the predicted mass loss by the method using transferred electrical charge and arc energy as known parameters is in the highest degree of agreement with measured values of mass erosion caused by the short-circuit current interruptions. The second most accurate method is using the peak arc current and arcing time to calculate the mass loss during current interruptions. The accuracy of estimated mass loss for fixed contact by this method is even higher than other methods. This can be a matter of discussion, in particular considering the fact that using the first method needs to measure on-line arc voltage along with short-circuit current during current interruption. Assuming the limitations of measurement of the arc voltage, applying the method using arc current and arcing time as required input data seems to be more reasonable than other methods. However, depending upon the importance of the function of the circuit breaker used in high-priority point of the power network, applying the first method using arc energy and transferred electrical charge is proposed to achieve higher accuracy.

V. Conclusion

In order to verify the accuracy of different thermal stress indices used in literature, such as transferred electrical charge, current squared and arc energy to evaluate the mass erosion caused by short-circuit current interruption, two series of experiments with fixed arcing time and varied current amplitudes; and fixed current amplitude and varied arcing times have been carried out on two puffer type high voltage circuit breakers. The results indicate that there is no linear relationship between mass loss and known thermal stress indices. Moreover, it has been shown that none of the defined thermal stresses can solely determine the amount of mass erosion. As a result, two-parameter indices to evaluate the mass erosion are proposed. The most accurate prediction method of mass loss is obtained if arc energy and transferred electrical charge are used as input parameters. However, regarding the difficulties of online arc voltage measurement, the method using arc current and arcing time seems to provide adequate accuracy in evaluating mass erosion. The proposed method can be applied as a non-invasive online method to monitor the interruption chamber ageing and assess the remaining lifetime of interruption chamber of gas circuit breakers.

VI. Acknowledgment

The authors would like to express their thanks to G. Farsad and F. Ataei for their technical support and providing the opportunity to do experiments in high voltage laboratory of Pars Switch Co., and to R. Hashemlo, Mohammadi, H. Mohajeri, H. Asadi, M. Osanlo, A. Solati, M. Salehpoor, Bayati for their help in carrying out the experiments.

VII. References

[1] Cigre WG 13-03: "Life management of circuit-breakers’," *Technical brochure*, vol. 165, 2000.

[2] G. Balzer, T. Orlowska, M. Halfmann, C. Neumann, and A. Strnad, "Life cycle management of circuit-breakers by application of reliability centered maintenance," *CIGRE 2000 Session*, pp. 13-103, 2000.

[3] A. A. Razi-Kazemi, M. Vakilian, K. Niayesh, and M. Lehtonen, "Data Mining of Online Diagnosed Waveforms for Probabilistic Condition Assessment of SF_6 Circuit Breakers," *IEEE Transactions on Power Delivery*, vol. 30, no. 3, pp. 1354-1362, 2015.

[4] A. A. Razi-Kazemi, M. Vakilian, K. Niayesh, and M. Lehtonen, "Circuit-breaker automated failure tracking based on coil current signature," *IEEE Transactions on Power Delivery*, vol. 29, no. 1, pp. 283-290, 2014.

[5] Cigre WG, "The first international enquiry on circuit-breaker failures and defects in service," *Electra 79*, 1981.

[6] Cigre WG, "Final report of the second international enquiry on high voltage circuit breaker failures and defects in service," *Paris, August/September*, 1994.

[7] A. Carvalho *et al.*, "Final Report of the 2004–2007 International Enquiry on Reliability of High Voltage Equipment," *Electra*, vol. 264, pp. 49-53, 2012.

[8] K. Niayesh and M. Runde, *Power Switching Components*. Springer, 2017.

[9] Z. Zhang, J. Zhang, E. Gockenbach, and H. Borsi, "Life management of SF 6 circuit breakers based on monitoring and diagnosis," *IEEE Electrical Insulation Magazine*, vol. 25, no. 3, pp. 21-29, 2009.

[10] M. Runde, G. Ottesen, B. Skyberg, and M. Ohlen, "Vibration analysis for diagnostic testing of circuit-breakers," *IEEE Transactions on power Delivery*, vol. 11, no. 4, pp. 1816-1823, 1996.

[11] A. Ukil, M. Zlatanski, and M. Hochlehnert, "Monitoring of HV generator circuit breaker contact ablation based on acoustic emission," *IEEE Transactions on Instrumentation and Measurement*, vol. 62, no. 10, pp. 2683-2693, 2013.

[12] M. Landry, O. Turcotte, and F. Brikci, "A complete strategy for conducting dynamic contact resistance measurements on HV circuit breakers," *IEEE Transactions on Power Delivery*, vol. 23, no. 2, pp. 710-716, 2008.

[13] A. Bhole and W. Gandhare, "An overview of dynamic contact resistance measurement of HV circuit breakers," *Journal of The Institution of Engineers (India): Series B*, vol. 97, no. 2, pp. 219-226, 2016.

[14] G. Chen, L. Lan, Z. Pan, X. Wen, Y. Wang, and Y. Wu, "Electrical erosion test and condition assessment of SF6 CB contact sets," *IET Generation, Transmission & Distribution*, vol. 11, no. 8, pp. 1901-1909, 2017.

[15] M. Khoddam, J. Sadeh, and P. Pourmohamadiyan, "Performance evaluation of circuit breaker electrical contact based on dynamic resistance signature and using health index," *IEEE Transactions on Components, Packaging and Manufacturing Technology*, vol. 6, no. 10, pp. 1505-1512, 2016.

[16] A. Pons, A. Sabot, and G. Babusci, "Electrical endurance and reliability of circuit-breakers-common experience and practice of two utilities," *IEEE Transactions on Power Delivery*, vol. 8, no. 1, pp. 168-174, 1993.

[17] J. Tepper, M. Seeger, T. Votteler, V. Behrens, and T. Honig, "Investigation on erosion of Cu/W contacts in high-voltage circuit breakers," *IEEE Transactions on Components and Packaging Technologies*, vol. 29, no. 3, pp. 658-665, 2006.

[18] A. Bagherpoor, S. Rahimi-Pordanjani, A. A. Razi-Kazemi, and K. Niayesh, "Online Condition Assessment of Interruption Chamber of Gas Circuit Breakers Using Arc Voltage Measurement," *IEEE Transactions on Power Delivery*, vol. 32, no. 4, pp. 1776-1783, 2017.

[19] W. Wilson, "High-current arc erosion of electric contact materials," *Transactions of the American Institute of Electrical Engineers. Part III: Power Apparatus and Systems*, vol. 74, no. 3, pp. 657-664, 1955.

[20] J. J. Shea, "Erosion and resistance characteristics of AgW and AgC contacts," *IEEE Transactions on Components and Packaging Technologies*, vol. 22, no. 2, pp. 331-336, 1999.

[21] J. J. Shea, "High current AC break arc contact erosion," in *Electrical Contacts, 2008. Proceedings of the 54th IEEE Holm Conference on*, 2008, pp. xxii-xlvi: IEEE.